




Article

Synthesis and Photophysical Properties of α -(*N*-Biphenyl)-Substituted 2,2'-Bipyridine-Based Push–Pull Fluorophores

Ekaterina S. Starnovskaya^{1,2}, Dmitry S. Kopchuk^{1,2}, Albert F. Khasanov¹ , Olga S. Taniya¹, Igor L. Nikonov^{1,2} , Maria I. Valieva^{1,2}, Dmitry E. Pavlyuk¹, Alexander S. Novikov^{3,4} , Grigory V. Zyryanov^{1,2,*} and Oleg N. Chupakhin^{1,2}

¹ Chemical Engineering Institute, Ural Federal University, 19 Mira St., Yekaterinburg 620002, Russia

² I. Ya. Postovsky Institute of Organic Synthesis of RAS, Ural Division, 22/20 S. Kovalevskoy/Akademicheskaya St., Yekaterinburg 62099, Russia

³ Institute of Chemistry, Saint Petersburg State University, 7/9 Universitetskaya Nab., Saint Petersburg 199034, Russia

⁴ Research Institute of Chemistry, Peoples' Friendship University of Russia (RUDN University), 6 Miklukho-Maklaya St., Moscow 117198, Russia

* Correspondence: gvzyryanov@gmail.com



Citation: Starnovskaya, E.S.; Kopchuk, D.S.; Khasanov, A.F.; Taniya, O.S.; Nikonov, I.L.; Valieva, M.I.; Pavlyuk, D.E.; Novikov, A.S.; Zyryanov, G.V.; Chupakhin, O.N. Synthesis and Photophysical Properties of α -(*N*-Biphenyl)-Substituted 2,2'-Bipyridine-Based Push–Pull Fluorophores. *Molecules* **2022**, *27*, 6879. <https://doi.org/10.3390/molecules27206879>

Academic Editor: Anna Cleta Croce

Received: 23 September 2022

Accepted: 11 October 2022

Published: 13 October 2022

Publisher's Note: MDPI stays neutral with regard to jurisdictional claims in published maps and institutional affiliations.



Copyright: © 2022 by the authors. Licensee MDPI, Basel, Switzerland. This article is an open access article distributed under the terms and conditions of the Creative Commons Attribution (CC BY) license (<https://creativecommons.org/licenses/by/4.0/>).

Abstract: A series of new α -(*N*-biphenyl)-substituted 2,2'-bipyridines were obtained through the combination of the ipso-nucleophilic aromatic substitution of the C5-cyano group, aza-Diels–Alder and Suzuki cross-coupling reactions, starting from 5-cyano-1,2,4-triazines. For the obtained compounds, photophysical and fluorosolvatochromic properties were studied. Fluorophores **3l** and **3b** demonstrated unexpected AIEE activity, while **3a** and **3h** showed promising nitroexplosive detection abilities.

Keywords: α -(*N*-Biphenyl)-substituted 2,2'-bipyridines; “push–pull” fluorophores; fluorescence; fluorosolvatochromic properties; Lippert–Mataga equation; AIEE; Hammett constants; nitroexplosive detection

1. Introduction

Compounds based on α -arylamino-2,2'-bipyridines and their fused analogs have already found wide practical applications. In particular, they serve as promising drug candidates, such as tyrosine kinases [1–3] or cyclooxygenase [4] modulators, and as promising candidates for the treatment of Lysosomal Storage Diseases (LSDs) [5] and other applications. In addition, α -arylamino-2,2'-bipyridines and their derivatives were reported as ligands for the transition metal complexes exhibiting promising photoluminescent behavior [6–9]. Several *N*-arylamino-substituted 2,2'-bipyridines reported as components for electroluminescent devices [10] and OLED systems [11]. In addition, platinum (II) or palladium (II) complexes based on *N*-aryl-(2,2'-bipyridin-6-yl)amines were reported as reagents for the photodynamic therapy of lung and prostate cancers [12,13] (Figure 1). Several isomeric amino-substituted 2,2'-bipyridines were reported as fluorescent indicators for Zn (II) and fluorescent dyes for the imaging of prostate cells [14]. Finally, arylamino-2,2'-bipyridines were reported as convenient synthons for the construction of various fused polynuclear systems [15–17].

Despite the extensive scope of practical applications for arylamino-substituted 2,2'-bipyridines, approaches for their synthesis are very limited. For instance, amination reactions via ipso-nucleophilic aromatic substitution of leaving groups, which are mainly halogen atoms, have become a most widely used methodology. Thus, interactions of mono- and dichloro-1,10-phenanthrolines with aniline or *p*-phenylenediamine have been described [16,18]. Another approach involves a deoxygenative amination of azine-*N*-oxides

with acyl azides via a [3 + 2] cycloaddition reaction [19]. Finally, the Pd-catalyzed Buchwald–Hartwig amination reaction was involved in case of interactions between bromine-/chloro-substituted bipyridines or terpyridines and aromatic (di)amines. As a result, various mono- and bis-arylamino-2,2'-bipyridines were obtained [6,13,17,20].

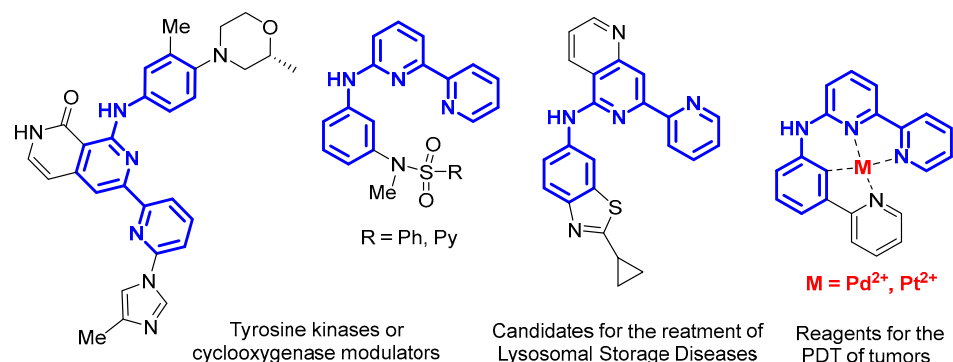


Figure 1. Examples of biologically active α -arylamino-2,2'-bipyridines [2,4,5,12].

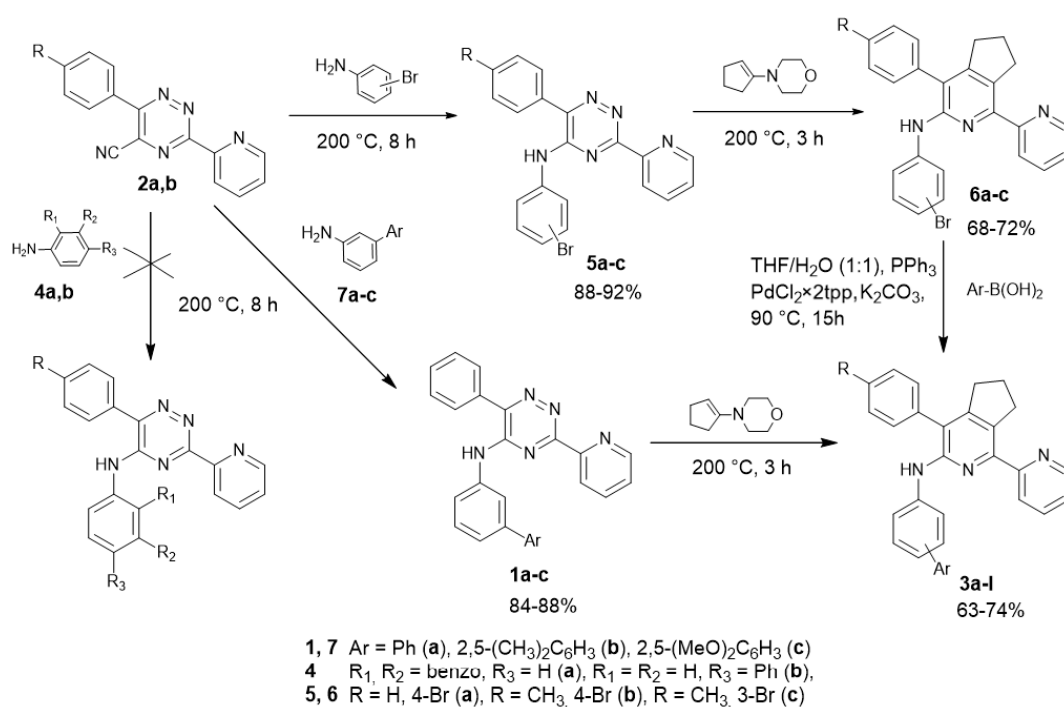
Recently, our group reported a more rational methodology for the preparation of α -arylamino-2,2'-bipyridines as promising push–pull fluorophores [21–23]. This methodology involved a transition metal-free (TM-free) direct ipso-amination of 3-(pyridin-2-yl)-5-cyano-1,2,4-triazines under the action of various anilines, including fluorine-substituted ones, in solvent-free conditions upon heating. A subsequent solvent-free aza-Diels–Alder reaction between C5-arylamino-substituted 1,2,4-triazines with 1-morpholinocyclopentene and 2,5-norbornadiene leads to the formation of target arylamino-substituted 2,2'-bipyridine. In this work, we wish to report a modification of the above-mentioned approaches to introduce the residues of [1,1'-biphenyl]-4-amine into the 1,2,4-triazine core [24] with the following, obtaining α -(*N*-biphenyl)-substituted 2,2'-bipyridines as push–pull fluorophores.

2. Results and Discussion

2.1. Synthesis of α -(*N*-Biphenyl)-Substituted 2,2'-Bipyridines 3a–l

As a first step, *N*-(biphenyl-3-yl)-1,2,4-triazines **1a–c** were prepared in 84–88% yields according to a previously described procedure [24] through ipso-nucleophilic aromatic substitution of the C5-cyano group in the reaction of 5-cyano-1,2,4-triazines **2a,b** and [1,1'-biphenyl]-3-amines in solvent-free conditions. The following aza-Diels–Alder reaction between them thus obtained C5-amino-substituted 1,2,4-triazines **1** with 1-morpholinocyclopentene afforded cyclopentane-fused 2,2'-bipyridines **3a–c** in 67–74% yields (Scheme 1).

Some limitations of the herein-reported method should be mentioned. Previously we were unable to introduce residues of [1,1'-biphenyl]-4-amines **4a,b** into the 1,2,4-triazine core [24]. A possible reason for the low reactivity of 4-aminobiphenyls is the high delocalization of the electron pair of the nitrogen atom due to the resonance with the extended polyaromatic system. In this regard, we developed an alternative approach towards α -arylamino-2,2'-bipyridines **3a–l** based on the use of commercially available 3- and 4-bromoanilines. As a result, the ipso-nucleophilic aromatic substitution of the C5-cyano group in 1,2,4-triazines resulted in the formation of intermediate products **5a–c**, while subsequent aza-Diels–Alder reactions resulted in bromoarene-substituted 2,2'-bipyridines **6a–c**. The final products **3a–l** were obtained due to Suzuki cross-coupling reactions between 2,2'-bipyridines **6a–c** and the corresponding arylboronic acid. In this case, the choice of the solvent system turned out to be important for the success of the cross-coupling reaction. In particular, it was not possible to satisfactorily obtain product **3** by a fairly traditional mixture of toluene, water, and ethanol, and a large number of unidentified impurities were presented in the reaction mixture. However, in a THF:water = 1:1 mixture this reaction proceeded smoothly to afford the desired products in up to 74% yields.



Scheme 1. Synthetic routes toward **3a-l**.

The structures of the products **3a-l** were confirmed by the data of ¹H and ¹³C NMR spectroscopy, as well as mass spectrometry and elemental analysis. Thus, in ¹H NMR spectra of the obtained products, the signals of protons of the 2-pyridyl residue, bipyridine aromatic substituents and biphenyl fragments, as well as a broadened singlet of the N-H group proton in the region of 6.72–7.04 ppm, were observed. In addition, the structure of key 2,2'-bipyridine **3a** was confirmed by means of single crystal X-ray diffraction analysis (Figure 2). According to the X-ray data, compound **3a** crystallizes in the centrosymmetric space group of the monoclinic system. The bond distances and angles in the molecule are near standard values. The molecule is nonplanar and only the bipyridine atoms are placed in a plane with trans-placed nitrogen atoms. The nitrogen atom of the diarylamino-moiety is planar and the NH-group is not involved in the formation of the H-bond. No significantly shortened intermolecular contacts in the crystal were observed.

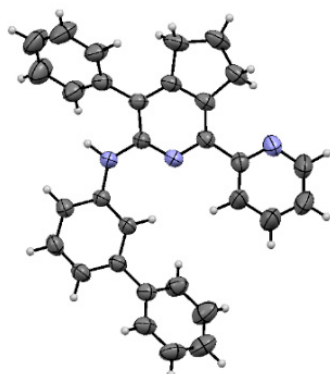


Figure 2. Structure of compound **3a** based on X-ray diffraction data.

2.2. Photophysical Studies

As a next step, the photophysical properties of the obtained α -biphenylamino-2,2'-bipyridines **3a-l** were studied (Table 1 and Table S1; Figure 3 and Figure S31). These compounds exhibited an intense blue-to-green fluorescence with emission maxima in the range of 443–505 nm and fluorescence quantum yields up to 49.1% in THF solutions.

Compared to previously described unsubstituted analogs (Table 1, Entries 1–4 and 12–15), as well as 3- and 4-bromophenyl-substituted precursors (Entries 11 and 22, 23), the extension of the conjugation system in the aniline moieties in **3a–l** expectedly redshifted the emission maxima with the highest values in the case of 4-biphenylamino derivatives. The Stokes shift values are either the same level as described earlier, or significantly exceed them and can reach up to 9670.29 cm^{-1} or 169 nm (Entry 10). This difference is very significant compared to α -phenylamino 2,2'-bipyridines (Entry 1 and 12). The highest quantum yields among all the products were observed for compound **3a** (49%, Entry 5), **3b** (48%, Entry 16), and **3d** (44%, Entry 18), functionalized at the *meta*-position of the aniline unit. These values are comparable with the quantum yields of α -arylamino-2,2'-bipyridines that are not functionalized with additional aromatic moieties. However, a significant decrease in quantum yields was observed in the case of some *para*-substituted derivatives (Entries 8–10).

Table 1. Photophysical properties of α -arylamino-2,2'-bipyridines **3a–l** in THF solution.

Entry	Ref./Comp.	Ar	R	$\lambda_{\text{abs max}}^a, \text{nm}$	ϵ_{M} , $\text{M}^{-1} \times \text{cm}^{-1}$	$\lambda_{\text{em max}}^b, \text{nm}$	Stokes Shift, cm^{-1}	Φ_{f} , % ^c
1	[22]		H	258, 285, 354	N/A	446	5827	46
2	[22]		2-MeO	259, 309, 359	N/A	453	5780	28
3	[22]		3-Cl	351	N/A	427	5070	55
4	[22]		4-Me	259, 287, 359	N/A	469	6533	28
5	3a		3-Ph	251, 356	35,200	443	5516	49
6	3e	Ph	3-(2,5-(MeO) ₂ C ₆ H ₄)	295, 350 (sh)	34,300	450	6349	19
7	3f		3-(2,5-Me ₂ C ₆ H ₄)	287, 356	42,000	448	5768	39
8	3h		4-Ph	269, 313, 354 (sh)	21,000	466	6789	32
9	3k		4-(4-MeOC ₆ H ₄)	317, 352 (sh)	19,400	484	7747	2
10	3l		4-(4-Ph ₂ NC ₆ H ₄)	289, 342	60,500	511	9670	3
11	6a		4-Br	259, 299, 353	28,300	441	5652	30
12	[22]		H	295, 356	N/A	445	5617	48
13	[22]		4-CN	316	N/A	417	7664	45
14	[22]		4-MeO	262, 289 (sh), 362	N/A	498	7543	4
15	[23]		4-F	257, 282 (sh), 353	N/A	447	5957	53
16	3b		3-(4-Ph ₂ NC ₆ H ₄)	297, 335 (sh)	21,100	444	7328	48
17	3c	Tol	3-(3,4,5-(MeO) ₂ C ₆ H ₂)	259, 356	49,800	448	5768	38
18	3d		3-(4-MeOC ₆ H ₄)	356	7700	446	5668	44
19	3g		3-(4-Et ₂ NC ₆ H ₄)	299, 360 (sh)	8000	452	5653	33
20	3i		4-(3,4,5-(MeO) ₃ C ₆ H ₂)	317, 360 (sh)	17,000	472	6591	26
21	3j		4-(4-MeOC ₆ H ₄)	270, 314, 358 (sh)	16,900	479	7056	21
22	6b		4-Br	263, 287, 354	18,400	440	5521	29
23	6c		3-Br	263 (sh), 283, 351	13,900	426	5015	45

^a Absorption spectra were measured at r.t. in the THF solution in a range from 200 to 600 nm. ^b Emission spectra were measured at r.t. in the THF solution. ^c Absolute quantum yields were measured by using the integrating sphere of the Horiba FluoroMax 4 spectrofluorometer at r.t. in the THF solution. The concentration for all fluorophores was 10^{-5} M .

It is worth noting the change in the photophysical properties of α -arylamino-2,2'-bipyridines bearing methoxy- (Entry 14) or 4-methoxyphenyl groups (Entry 21). In this case, the introduction of an additional 1,3-phenylene fragment into the bipyridine core results in a blueshift of the emission maximum by 19 nm and the reduction of the Stokes shift value (7543.99 cm^{-1} vs. 7056.13 cm^{-1}). However, fluorescence quantum yield increased from 4% to 21%. Therefore, the introduction of additional aromatic substituents into the α -aniline fragment of the 2,2'-bipyridine core could be used as a tool to tune the photophysical properties and is of particular interest.

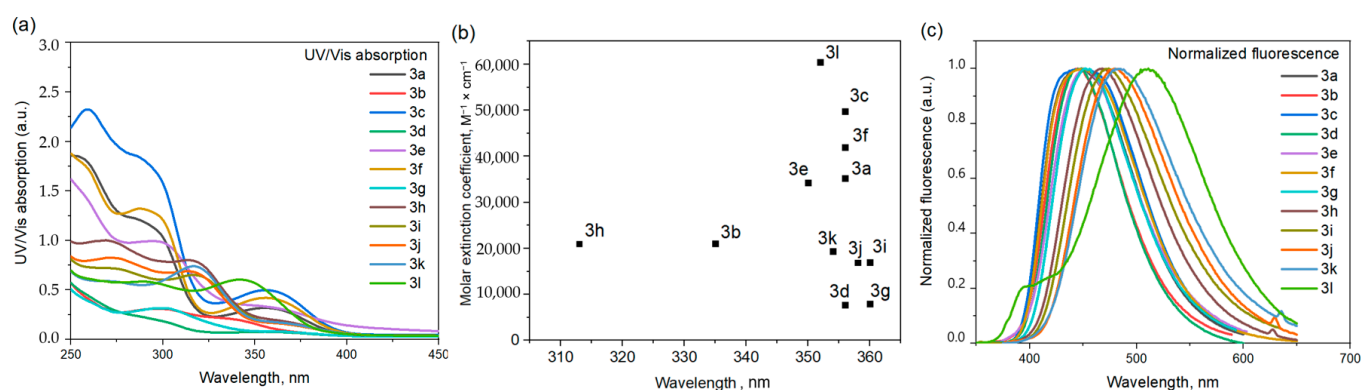


Figure 3. UV/Vis spectra (a), molar extinction coefficient, and (b) normalized fluorescence (c) spectra for **3a–l** in THF solutions at room temperature. The concentration of all fluorophores was 10^{-5} M.

2.3. Studies of Fluorosolvatochromism

In our recent works, we have already demonstrated a well-pronounced fluorosolvatochromic behavior of 2,2'-bipyridines functionalized with donor substituents, including aniline residues [22,23,25,26]. The herein-reported compounds **3a–l** also exhibited a pronounced fluorosolvatochromism, which was demonstrated for the most representative compounds **3b,g,i,l** (Figure 4, Figure 5 and Figures S32–S35).

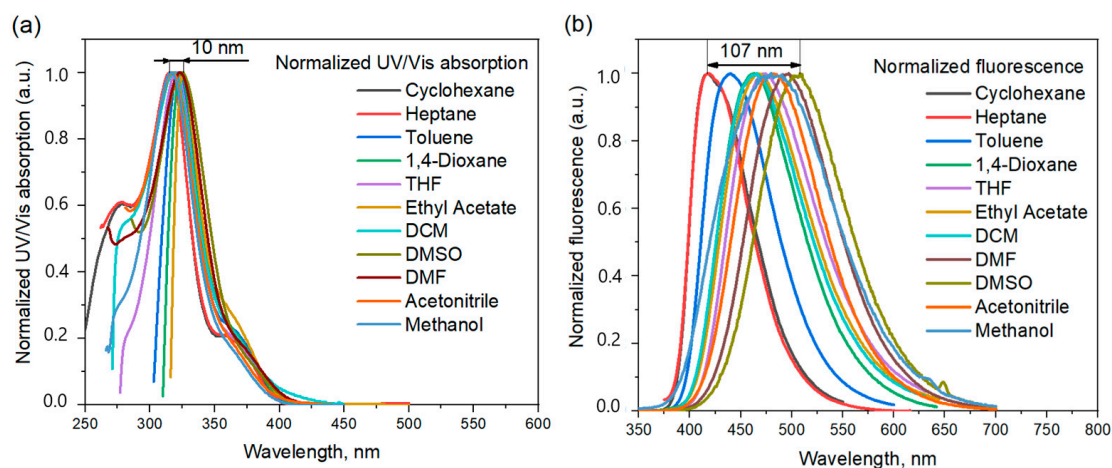


Figure 4. UV/Vis (a) and fluorescence (b) spectra of **3i** in different solvents at room temperature.

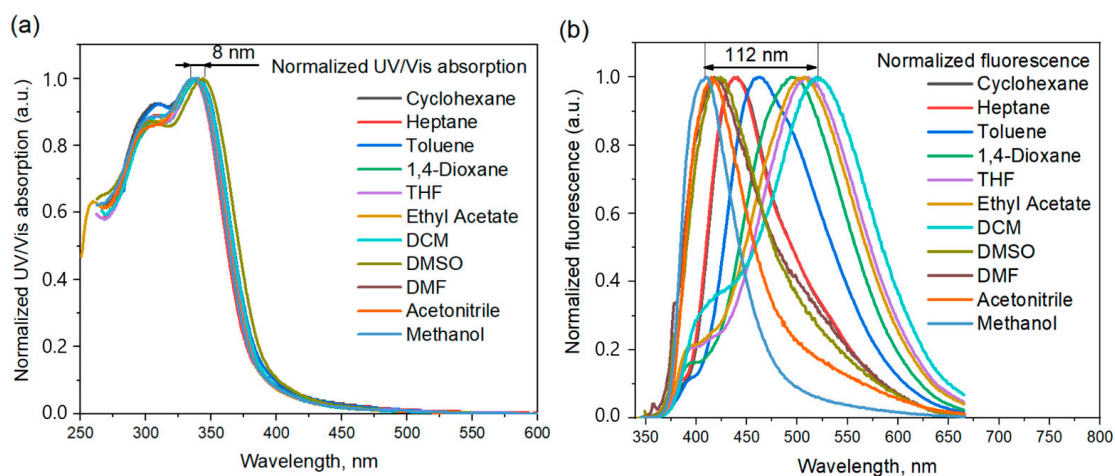


Figure 5. UV/Vis (a) and fluorescence (b) spectra of **3l** in different solvents at room temperature.

Solvent polarity did not significantly affect the absorption spectra, while it influenced significantly the fluorescence spectra of the fluorophores **3b,g,i,l** (Figures 4, 5 and S32–S35, Tables S2–S5). Thus, a gradual increase of the solvent polarity from cyclohexane to DMSO led to a gradual redshift of the fluorescence maxima with an increase of the Stokes shift values. For example, the observed fluorescence maximum for **3i** in cyclohexane was 438 nm, and the Stokes shift was 99 nm, while in DMSO these values were 515 nm and 176 nm, respectively. In the case of compound **3l**, the use of more polar solvents (DMF, acetonitrile and methanol) resulted in a blueshift of the emission maxima relative to the emission in DMSO, while in a solvent row from cyclohexane to dichloromethane, an increase of the solvent polarity exhibited a redshift of the emission maxima. It is worth mentioning that the difference between the largest and smallest values of the emission maximum, in the case of **3b,g,i,l** (69 nm, 67 nm, 107 nm and 112 nm, respectively, Figures S32–S35), is greater than the same difference (38–70 nm) for the previously reported aniline containing 2,2'-bipyridines [22,23].

To estimate the push–pull character of the obtained fluorophores, a mathematical analysis of the obtained experimental data was carried out using the Lippert–Mataga equation (Equation (1)) [27–29]. We found that the introduction of additional aromatic fragments into the aniline residue in compounds **3b,g,i,l** led to an increase in the difference between the dipole moments of the ground (μ_G) and excited (μ_E) states. As a result, we calculated $\Delta\mu$ for **3b,g,i,l** (Table 2). These values are relatively high for the 2,2'-bipyridine type fluorophores, second only to some examples (Figure S36) [22,25,26,30].

$$v_A - v_F = \frac{2}{hc} \left(\frac{\varepsilon - 1}{2\varepsilon + 1} - \frac{n^2 - 1}{2n^2 + 1} \right) \frac{(\mu_E - \mu_G)^2}{a^3} \quad (1)$$

Equation (1). In the Lippert–Mataga equation (v_A and v_F are the wavenumbers (cm^{-1}) of the absorption and emission, respectively, h is Planck's constant, c is the speed of light in vacuum, a is the radius of the cavity in which the fluorophore resides (4Å, [27]), μ_E and μ_G are the excited and ground state dipole moment, respectively.

Table 2. Differences between the calculated dipole moments $\Delta\mu$ of optimized equilibrium model structures **3b,g,i,l** in the ground, (S_0) excited, and (S_1) multiplicity states.

Compound	3b	3g	3i	3l
$\Delta\mu$, D	11.93	12.73	10.62	12.61

For a more detailed study of the effect of solvent polarity on the photophysical properties, a Lippert–Mataga plot was constructed, that is, the dependence of the Stokes shift (cm^{-1}) of the fluorophore on the orientational polarizability of the solvent (Δf). This plot indicated that **3b,g,i,l** demonstrated a linear dependence ($R^2 > 0.90$, Figure 6a and Table S6) only in the range of cyclohexane—DCM solvents—while in more polar solvents, the linearity was broken and there was a sharp drop in the Stokes shift values (Figure 6a, Table S7). Deviations from linearity in the Lippert–Mataga plots indicate the occurrence of some intermolecular interactions in these solvents, such as the hydrogen bonds formation, which is confirmed by a certain linearity in this case ($R^2 = 0.69 - 0.99$, Table S7), and can not be explained by traces of water in selected solvents due to the absence of these deviations in related α -arylamino-2,2'-bipyridines [22] (that is, the ones without the 1,3- or 1,4-phenylene unit). The protic nature of methanol could influence corresponding emission spectra as well. Thus, this unusual behavior is discussible.

$$\Delta f = \frac{\varepsilon - 1}{2\varepsilon + 1} - \frac{n^2 - 1}{2n^2 + 1} \quad (2)$$

Equation (2). The orientational polarizability of the solvent, where ε and n are the dielectric constant and the refraction index for the solvents, respectively.

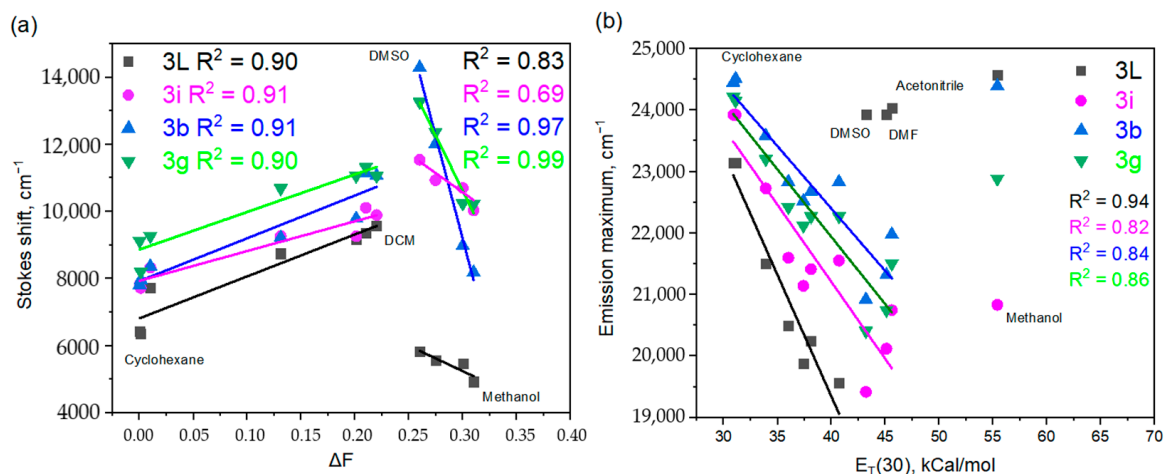


Figure 6. Lippert–Mataga plot (a) and the variation of the fluorescence emission maximum with the empirical solvent polarity parameter $E_T(30)$ (b) for the compounds **3b,g,i,l**.

The fluorosolvatochromism of **3b,g,i,l** correlates well with the solvent polarity scales according to Kosower [31,32] and Dimroth/Reichardt [33,34] (Table 3, parameters Z and $E_T(30)$, respectively), while some deviations were observed only in the case of the most polar solvents (DMF—methanol). Nevertheless, Figure 6b indicates that the dependence of the fluorescence maxima on the values of the empirical polarity factor $E_T(30)$ proceeds linearly ($R^2 > 0.82$, Tables S8), except for **3b,g,i** in methanol, as well as for **3l** in DMSO, DMF, acetonitrile, and methanol. This linear change in emission also confirms the phenomenon of fluorosolvatochromism (Table 3) [35].

Table 3. Emission maxima for compounds **3b,g,i,l** in different solvents and Z and $E_T(30)$ parameters for the solvents.

Solvent	Z , kcal/mol ⁻¹	$E_T(30)$, kcal/mol ⁻¹	$\lambda_{em} \text{ max, nm}$			
			3b	3g	3i	3l
Methanol	83.6	55.4	410	437	480	407
Acetonitrile	71.3	45.6	455	465	482	416
DMSO	71.1	45.1	469	474	497	418
DMF	68.4	43.2	478	480	515	418
DCM	64.7	40.7	438	449	464	519
Ethyl Acetate	59.4	38.1	444	452	467	511
THF	58.8	37.4	441	449	473	507
1,4-Dioxane	N/A	36.0	438	446	463	494
Toluene	N/A	33.9	424	431	440	463
<i>n</i> -Heptane	N/A	31.1	408	414	418	438
Cyclohexane	N/A	30.9	409	413	418	441

The electron-donating or accepting ability of organic substituents is an important parameter affecting not only their reactivity but also the pK_a of ionizable groups and chromophore properties. These substituent properties are usually described by Hammett sigma constants, constants obtained by the ionization of substituted benzoic acids. Although the values of these constants have been measured for the most common functional groups, data are not available for many important substituents. However, Peter Ertl published the results of a quantum chemical calculation of substituent descriptors compatible with Hammett sigma constants by using a more sophisticated methodology and a larger set of training data and presented a free web-based tool to calculate substituent descriptors compatible with Hammett sigma constants. This is available at: <https://peter-ertl.com/molecular/substituents/sigmas.html> (accessed on 16 May 2022) [36].

The dependence of emission maxima on Hammett sigma constants for two groups of α -biphenylamino-2,2'-bipyridine fluorophores, *para*- and *meta*-substituted with respect to the aniline residue, were plotted (Figure S37a,b). Except for **3g**, *meta*-substituted fluorophores **3a–f** showed an acceptor character (Figure S37a). At the same time, a good linear correlation with σ_m ($R^2 = 0.92$) was observed provided that such strongest electron-withdrawing substituents as Cl (#3) and Br (**5c**) are included in the analyzed sequence. For donor-substituted compounds **3j**, **3k**, **#4**, **#14** including the hydrogen-substituted compound **3h**, as well as acceptor-substituted compounds **5a**, **5b**, **#15**, **#13**, a well-linear correlation with σ_p ($R^2 = 0.89$) was observed (Figure S37b). Thus, the correlation analysis of long-wavelength emission maxima plotted as a function of the Hammett constants made it possible to obtain the relationship between the structure and photophysical properties of the resulting fluorophores.

2.4. DFT Studies

To understand the structure-photophysical properties relationship, we performed density functional theory (DFT) calculations with the help of the Gaussian-09 [37] program package at the B3LYP/6-31G**/PM6 level in acetonitrile (see Computational Details and Table S8 in Supplementary Materials) to obtain optimized molecular structures, energy levels of boundary molecular orbitals, dipole moments and molecular electrostatic potentials for the molecules **3b,g,i,l**. The HOMO-orbitals were distributed on the substituted biphenyl residues acting as electron donors, while LUMO-orbitals were distributed on the 2,2'-bipyridine cores acting as electron acceptors (Figure 7). This facilitates the intermolecular charge transfer (ICT) process (“push–pull” effect) in a molecule and correlates well with the photophysical experimental data. According to the calculation, the maximum difference between the dipole moments in the ground and excited states $\Delta\mu$ is more than 10D for the molecule **3l** (Table S9), which is typical for the ICT state [38]. However, there are significant differences in the $\Delta\mu$ values between those calculated and obtained via Lippert–Mataga equations for the rest of molecules **3b,g,i** (Table S9). The calculated values of the energy gaps (ΔE) correlate well with the UV spectroscopic data (Table S10 and Figure S38). Thus, a significant bathochromic shift of absorption maxima (289 nm and 342 nm) is observed in 4-diphenylaminophenyl-substituted compound **3l**, which is in a more favorable energy state ($\Delta E = 3.94$ eV (Figure 7)).

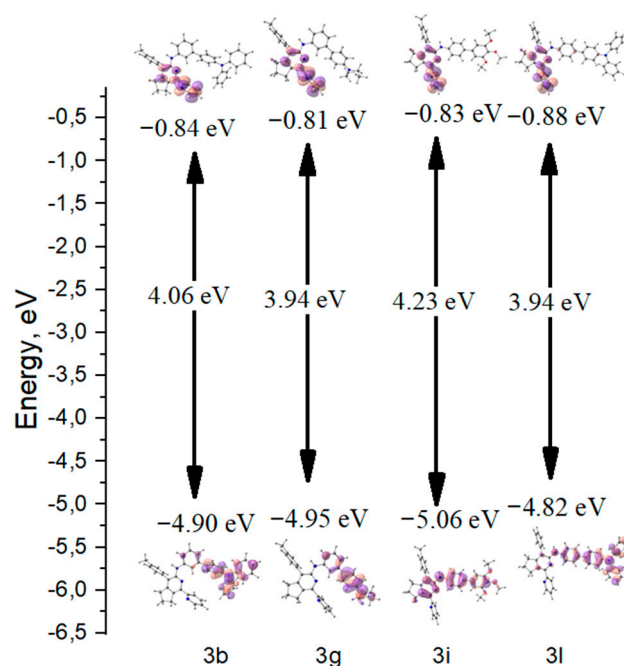


Figure 7. Frontier molecular orbitals and the energy level diagrams of **3b,g,i,l**.

In order to elucidate the electron transfer process for α -biphenylamino-2,2'-bipyridines, the molecular electrostatic potential (MEP) distribution (Table S9) was calculated. The results obtained also confirm that the electron transfer occurs from an electron-rich biphenylene unit to the electron-deficient 2,2'-bipyridine core leading to the “push–pull” process.

2.5. AIEE Properties

It was found that compound **3l** exhibits a pronounced aggregation-induced enhanced emission (AIEE) behavior (Figure 8a). With an increase of the water fraction (f_w) in a solution of **3l** in acetonitrile, a new emission band appeared with a maximum of 468 nm. The highest intensity was achieved at $f_w = 60\%$, while the further increase in f_w slightly decreased the emission intensity. This AIEE behavior is due to the presence of a triphenylamine moiety that realizes the restricted intramolecular rotation (RIR) mechanism, whereas fluorophores with any other groups at both *para*- and *meta*-positions did not demonstrate any AIEE activity, except **3b**. The **3b** molecule exhibited unusual behavior in the water-acetonitrile mixture. In this case, the emission maximum shifted from 482 nm to 492 nm at $f_w = 10\%$, accompanied by the quenching of fluorescence. However, a bathochromic shift from 460 nm to 492 nm was detected starting from $f_w = 70\%$, accompanied by an enhancement of the fluorescent emission, which reached a limit at $f_w = 80\%$ (Figure 8b). This peculiar behavior at $f_w = 0\text{--}70\%$ could be explained by the high polarity of water and at $f_w = 70\text{--}90\%$, by the formation of aggregates.

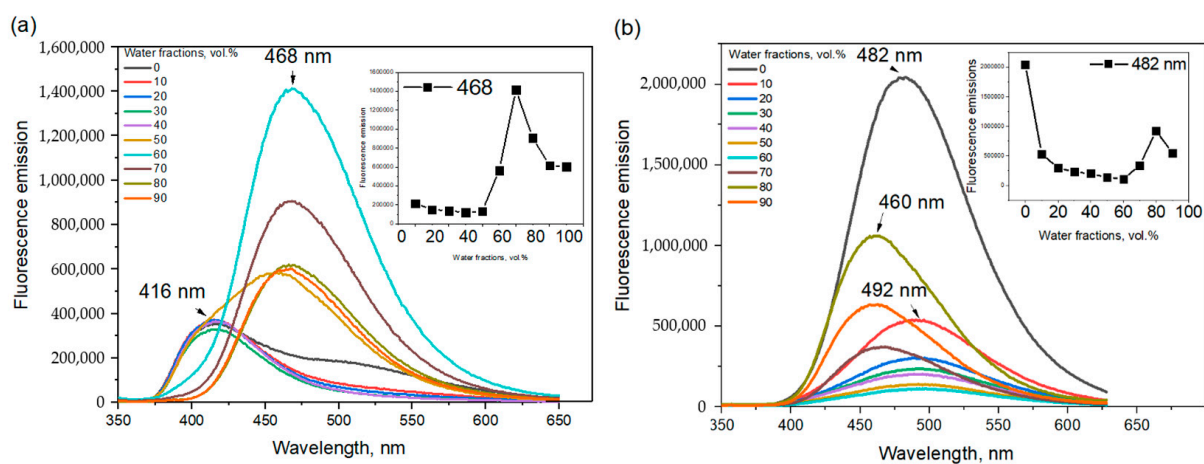


Figure 8. AIEE of **3l** (a) and **3b** (b) in acetonitrile-water mixtures (10^{-5} M concentration, room temperature, λ_{ex} 342 nm). Insets: (a) a plot of fluorescence intensity of **3l** at 468 nm at different f_w values (b) a plot of fluorescence intensity of **3b** at 482 nm at different f_w values.

2.6. Studies of Sensing Properties

Electron-rich π -conjugated azine fluorophores can act as sensors or probes for high electron-deficient nitroaromatic explosives via exhibiting photoinduced electron transfer (PET) from one molecule to another [39]. This process is accompanied by the quenching of the fluorescence of a sensor.

In this regard, fluorophores **3a,h** were chosen among the whole series of α -(*N*-biphenyl)-substituted 2,2'-bipyridine as model objects in the study of the sensory properties of these fluorophores in the detection of nitroaromatic explosives. The position of the phenyl ring in the aniline residue is the only difference between **3a** (*meta*) and **3h** (*para*) that will allow their comparative analysis. Picric acid (PA) and 2,4,6-trinitrotoluene (TNT) were chosen as the most typical analytes. To determine the efficiency of fluorescence quenching, the Stern–Volmer model was chosen as a well-known method for evaluating sensory properties. Fluorometric titration was performed by the single point methodology using a Horiba FluoroMax 4.

Based on the results of the fluorometric titration, Stern–Volmer plots (Figure 9) with corresponding quenching constants K_{SV} (Table 4, Equation (3)), as well as limits of detection (LOD) of nitroanalytes (Table 4, Equation (4)) were determined. Samples **3a,h** showed high K_{SV} (from 10.6 to 68.3 M^{-1}) and LOD (64.9 to 5535.5 ppb) values, which are in the same order as the described pyridine-based probes [40]. Probe **3a** demonstrated higher K_{SV} values and better sensitivity toward both PA and TNT resulting in a *meta*-position that is more promising for creating sensors and probes for nitroexplosive detection. Thus, α -(*N*-biphenyl)-substituted 2,2'-bipyridines may find a potential application as sensors/probes for the determination of nitroaromatic explosives.

$$\frac{I_0}{I} = 1 + K_{SV} \times [Q] \quad (3)$$

where I_0 is the fluorescence intensity in the absence of a nitroexplosive, I is the fluorescence intensity in the presence of a nitroexplosive, K_{sv} is the Stern–Volmer constant, $[Q]$ is the concentration of a nitroexplosive.

Equation (3). Stern–Volmer equation.

$$LOD = \frac{3 \times \sigma}{k} \quad (4)$$

where LOD is the limit of detection, σ is the standard deviation of the fluorophore intensity in the absence of a nitroexplosive, k is the slope of the linear calibration curve.

Equation (4). LOD calculation.

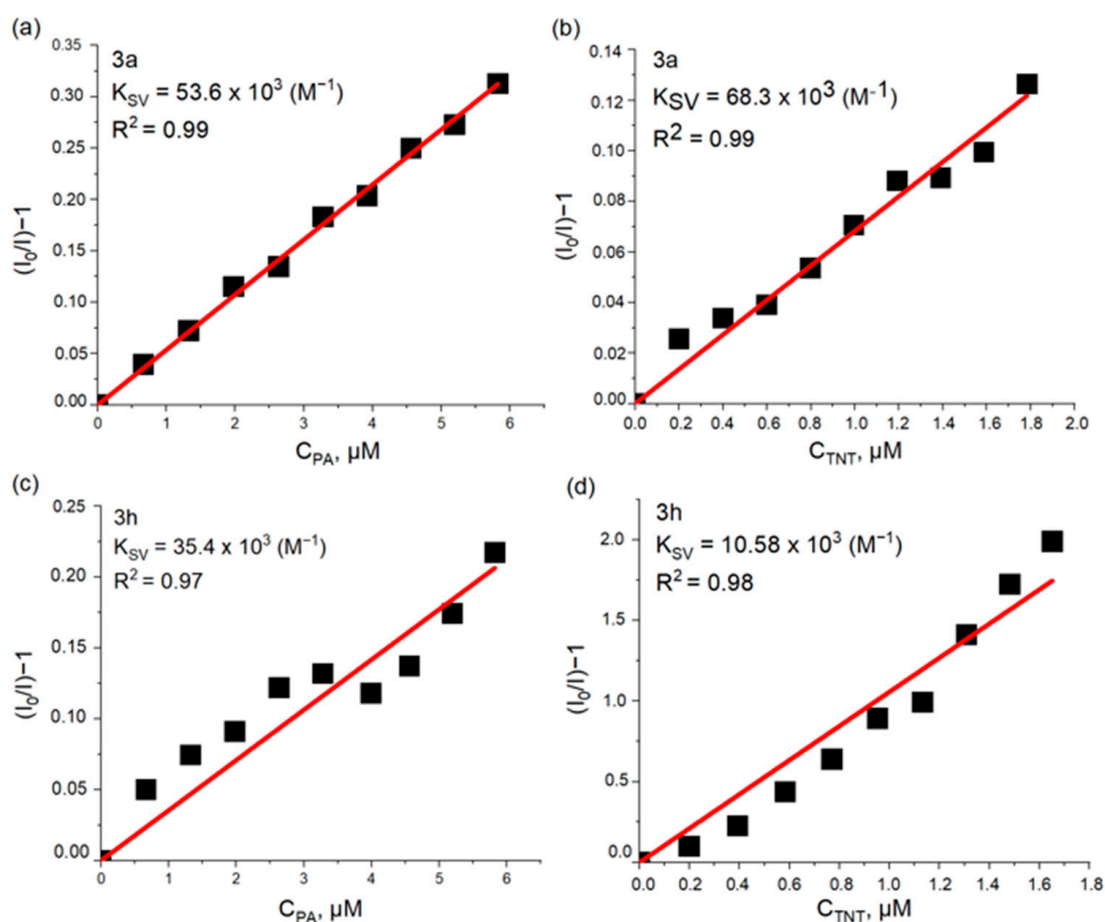


Figure 9. Stern–Volmer plots for the fluorescence quenching of **3a** in the presence of PA (a) and TNT (b), **3h** in the presence of PA (c) and TNT (d) in a media of THF. Concentrations of **3a** and **3h** are 10 μM , PA and TNT—200 μM . Obtained by the single point method.

Table 4. Stern–Volmer constants and LOD for the **3a** and **3h** sensors.

		3a	3h
PA	K_{SV}, M^{-1}	53.6	35.4
	LOD, ppb	139.6	480.3
TNT	K_{SV}, M^{-1}	68.3	10.6
	LOD, ppb	64.9	5535.5

3. Materials and Method

3.1. Materials and Equipment

Unless otherwise indicated, all common reagents and solvents were used from commercial suppliers without further purification. 6-Phenyl-3-(pyridin-2-yl)-1,2,4-triazine-5-carbonitrile **2a** and 6-(4-tolyl)-3-(pyridin-2-yl)-1,2,4-triazine-5-carbonitrile **2b** were synthesized according to reported literature [26,41].

Melting points were determined on Boetius combined heating stages. TLC and column chromatography were carried out on SiO₂. ¹H NMR and ¹³C NMR spectra were recorded at room temperature at 400 and 100 MHz, respectively, on a Bruker DRX-400 spectrometer using CDCl₃ or DMSO-*d*₆ as the solvent. Hydrogen chemical shifts were referenced to the hydrogen resonance of the corresponding solvent (DMSO-*d*₆, $\delta = 2.50$ ppm or CDCl₃, $\delta = 7.26$ ppm). Carbon chemical shifts were referenced to the carbon resonances of the solvent (CDCl₃, $\delta = 77.16$ ppm). Peaks were labeled as singlet (s), doublet (d), triplet (t), doublet of doublets (dd), doublet of doublets of doublets (ddd), and multiplet (m). Mass spectra were recorded on a MicrOTOF-Q II (Bruker Daltonics), electrospray as a method of ionization UV–vis absorption spectra were recorded on a Shimadzu UV-1800 spectrophotometer, and emission spectra were measured on a Horiba FluoroMax-4 by using quartz cells with a 1 cm path length at room temperature. Absolute quantum yields of the luminescence of target compounds in solution were measured by using the integrating sphere Quanta- ϕ of the Horiba FluoroMax 4 at room temperature.

3.2. General Method for the Synthesis of 5-Arylamino-1,2,4-Triazines **1a–c** and **5a–c**

The mixture of corresponding 5-cyano-1,2,4-triazine **2a,b** (1 mmol) and corresponding aniline (1.05 mmol) was stirred at 200 °C for 8 h under an argon atmosphere. The products were used in the next step without additional purification. Analytical samples were obtained by flash chromatography with chloroform as eluent.

3.3. General Method for the Synthesis of *N*-Aryl-1-(Pyridine-2-yl)-6,7-Dihydro-5H-Cyclopenta[*c*]pyridin-3-Amines **3a–l** and **6a–c**

The mixture of corresponding 5-arylamino-1,2,4-triazine **1a–c** (0.3 mmol) or **5a–c** and 1-morpholinocyclopentene (1.5 mmol) was stirred at 200 °C for 2 h under an argon atmosphere. Then, the additional portion of 1-morpholinocyclopentene (0.75 mmol) was added and the resulting mixture was stirred for an additional 1 h at the same conditions. The products were separated by flash chromatography (DCM as eluent) and were then purified by recrystallization (ethanol).

3.4. General Method for the Synthesis of *N*-Aryl-1-(Pyridine-2-yl)-6,7-Dihydro-5H-Cyclopenta[*c*]pyridin-3-Amines **3a–l** Via Suzuki Cross-Coupling Reaction

The corresponding compound **6a–c** (0.3 mmol) was dissolved in THF (15 mL), followed by the addition of the corresponding boronic acid (0.33 mmol), Pd(*tpp*)₂Cl₂ (6.3 mg, 0.009 mmol), triphenylphosphine (3.9 mg, 0.015 mmol), and solution of K₂CO₃ (415 mg, 3 mmol) in water (15 mL). The resulting mixture was stirred at 90 °C in an argon atmosphere for 24 h. After completion, the reaction mixture was extracted with ethyl acetate (10 mL). The organic phase was washed with an aqueous solution of KOH, ammonium chloride and water, and dried with anhydrous sodium sulfate. The solvent was removed

under reduced pressure. Ethanol was added to the residue and the obtained precipitate was filtered off, washed with ethanol, and dried.

3.5. Crystallography

The XRD analysis was carried out using equipment at the Center for Joint Use “Spectroscopy and Analysis of Organic Compounds” at the Postovsky Institute of Organic Synthesis of the Russian Academy of Sciences (Ural Branch). The experiments were accomplished on an automated X-ray diffractometer Xcalibur 3 with CCD detector using a standard procedure (MoK α -irradiation, graphite monochromator, ω -scans with 1 σ step at T = 295(2) K). Empirical absorption correction was applied. The solution and refinement of the structures were accomplished using the Olex program package [42]. The structures were solved by the method of the intrinsic phases in ShelXT program and refined by ShelXL by the full-matrix least-squared method for non-hydrogen atoms [43]. The H-atoms at C-H bonds were placed in the calculated positions, and the H-atoms at N-H bonds were refined independently in isotropic approximation.

The result of the X-ray diffraction analysis for compound **3a** was deposited with the Cambridge Crystallographic Data Centre (CCDC 2167697) and can be found in supporting documents.

4. Conclusions

In conclusion, a rational synthetic approach toward α -biphenylamino-2,2'-bipyridines push-pull fluorophores starting from 5-cyano-1,2,4-triazines precursors using the sequence of the ipso-nucleophilic aromatic substitution of the cyano group, aza-Diels–Alder reaction and Suzuki cross-coupling was reported. In the THF solutions, the herein-reported fluorophores exhibited an intensive emission with a maxima of up to 511 nm along with up to 49.1% quantum yields. The most representative fluorophores **3b,g,i,l** exhibited a well-pronounced positive fluorosolvatochromic behavior, which was well correlated with the solvent polarity scales according to Kosower and Dimroth/Reichardt as well as Lippert–Mataga mathematical models. DFT calculations confirmed the presence of the ICT state of the fluorophores. Fluorophores **3l** and **3b** demonstrated an unexpected AIEE activity, while fluorophores **3a** and **3h** exhibited sensing properties toward nitroaromatics (explosives) with high K_{sv} and LOD values.

Supplementary Materials: The following supporting information can be downloaded at: <https://www.mdpi.com/article/10.3390/molecules27206879/s1>, Figures S1–S30: ¹H and ¹³C NMR spectra of compounds **5a–c**, **6a–c**, **3a–l**; Figure S31: Absorption and emission spectra of **3a–l** and **5a–c** in THF; Figure S32: Normalized fluorescence emission spectra of **3b** in different solvents; Figure S33: Normalized fluorescence emission spectra of **3g** in different solvents; Figure S34: Normalized fluorescence emission spectra of **3i** in different solvents; Figure S35: Normalized fluorescence emission spectra of **3l** in different solvents; Figure S36: Difference in dipole moments ($\Delta\mu$) of some 2,2'-bipyridine derivatives and analogs calculated according to Lippert–Mataga equation; Figure S37: Plot of the Hammett constants at the meta (a) and para (b) position versus the values of the fluorophore emission maxima; Figure S38: Tauc Plots for **3b,g,i,l** constructed based on UV/Vis data; Table S1: Selected bond lengths and angles for compound **3a**; Table S2: Orientation polarizability for solvents (Δf), absorption and fluorescence emission maxima (λ_{abs} , λ_{em} , nm) and Stokes shift (nm, cm^{-1}) of **3b** in different solvents; Table S3: Orientation polarizability for solvents (Δf), absorption and fluorescence emission maxima (λ_{abs} , λ_{em} , nm) and Stokes shift (nm, cm^{-1}) of **3g** in different solvents; Table S4: Orientation polarizability for solvents (Δf), absorption and fluorescence emission maxima (λ_{abs} , λ_{em} , nm) and Stokes shift (nm, cm^{-1}) of **3i** in different solvents; Table S5: Orientation polarizability for solvents (Δf), absorption and fluorescence emission maxima (λ_{abs} , λ_{em} , nm) and Stokes shift (nm, cm^{-1}) of **3l** in different solvents; Table S6: Data for the Lippert–Mataga plots of **3b,g,i,l**; Table S7: Data for the Lippert–Mataga plots of **3b,g,i,l** in the range of polar solvents (DMSO, DMF, acetonitrile, methanol); Table S8: Data for fluorescence emission maximum relationship with the empirical solvent polarity parameter ET(30) plots; Table S9: Molecular electrostatic potential energy map and calculated dipole moments (in Debye) in ground (S₀) and excited (S₁) multiplicity states for **3b,g,i,l**; Table S10:

HOMO-LUMO Energy levels for fluorophores **3b,g,i,l** in a gas phase. Reference [44] has been cited in the Supplementary Materials.

Author Contributions: Conceptualization, D.S.K.; Data curation, O.S.T.; Formal analysis, I.L.N.; Funding acquisition, A.F.K. and G.V.Z.; Investigation, E.S.S., M.I.V., D.E.P. and A.S.N.; Methodology, E.S.S.; Project administration, O.N.C.; Validation, D.S.K., A.F.K. and O.S.T.; Visualization, A.F.K.; Writing—original draft, A.F.K.; Writing—review and editing, D.S.K. and G.V.Z. All authors have read and agreed to the published version of the manuscript.

Funding: This research was funded by the Russian Scientific Foundation, grant number 19-73-10144-P dated 2 August 2022 (Photophysical Studies and Studies of Fluorosolvatochromism) and 21-13-00304 dated 19 April 2021 (AIEE Studies)), by the Grants Council of the President of the Russian Federation (grant number NSH- 1223.2022.1.3, state contract № 075-15-2022-802 dated 6 May 2022) and the RUDN University Strategic Academic Leadership Program.

Institutional Review Board Statement: Not applicable.

Informed Consent Statement: Not applicable.

Data Availability Statement: The data presented in this study are available on request from the corresponding author and co-authors.

Conflicts of Interest: The authors declare no conflict of interest.

Sample Availability: Samples of the compounds α -(N-Biphenyl)-Substituted 2,2'-Bipyridine are available from the authors.

References

1. Okram, B.; Uno, T.; Ding, Q.; Liu, Y.; Jin, Y.; Jin, Q.; Wu, X.; Che, J.; Yan, S.F.; Hao, X. Compounds and Compositions as Kinase Inhibitors. U.S. Patent No. 12/865,339, 14 May 2008.
2. De Lucca, G.V.; Shi, Q.; Liu, C.; Duan, J.; Tebben, A.J. Nicotinamide Compounds Useful as Kinase Modulators. U.S. Patent No. 8,586,751, 19 November 2013.
3. Towner, J.S.; Nichol, S.T.; Comer, J.A.; Ksiiazek, T.G.; Rollin, P.E. Human Ebola Virus Species and Compositions and Methods Thereof. U.S. Patent 20120251502A1, 24 October 2008.
4. Velcheva, M.; Vidmar, J.; Quandt, J. Vagation in Plants. U.S. Patent 2011/017203 A1, 26 May 2011.
5. Chen, B.; Finkel, T.; Liu, Y. Methods and Materials for Increasing Transcription Factor Eb Polypeptide Levels. U.S. Patent No. 17/420,597, 26 July 2019.
6. Dahl, E.W.; Szymczak, N.K. Hydrogen Bonds Dictate the Coordination Geometry of Copper: Characterization of a Square-Planar Copper(I) Complex. *Angew. Chem. Int. Ed.* **2016**, *55*, 3101–3105. [[CrossRef](#)] [[PubMed](#)]
7. Carroll, J.; Gagnier, J.P.; Garner, A.W.; Moots, J.G.; Pike, R.D.; Li, Y.; Huo, S. Reaction of N-Isopropyl-N-Phenyl-2,2'-Bipyridin-6-Amine with K₂PtCl₄: Selective C–H Bond Activation, C–N Bond Cleavage, and Selective Acylation. *Organometallics* **2013**, *32*, 4828–4836. [[CrossRef](#)]
8. Huo, S.; Harris, C.F.; Vezzu, D.A.K.; Gagnier, J.P.; Smith, M.E.; Pike, R.D.; Li, Y. Novel Phosphorescent Tetradentate Bis-Cyclometalated C[∞]C * N[∞]N-Coordinated Platinum Complexes: Structure, Photophysics, and a Synthetic Adventure. *Polyhedron* **2013**, *52*, 1030–1040. [[CrossRef](#)]
9. Garner, A.W.; Harris, C.F.; Vezzu, D.A.K.; Pike, R.D.; Huo, S. Solvent-Controlled Switch of Selectivity between Sp² and Sp³ C–H Bond Activation by Platinum (ii). *Chem. Commun.* **2011**, *47*, 1902–1904. [[CrossRef](#)] [[PubMed](#)]
10. Smith, G.; Massare, J.M.; Tian, J.-H. Coronavirus Vaccine Formulations. U.S. Patent KR102080738 B1, 23 March 2021.
11. Ehrlich, G.; Fenster, M. Methods and Systems of Prioritizing Treatments, Vaccination, Testing and/or Activities while Protecting the Privacy of Individuals. U.S. Patent 2021/230197, 31 August 2021.
12. Vezzu, D.A.K.; Lu, Q.; Chen, Y.-H.; Huo, S. Cytotoxicity of Cyclometalated Platinum Complexes Based on Tridentate NCN and CNN-Coordinating Ligands: Remarkable Coordination Dependence. *J. Inorg. Biochem.* **2014**, *134*, 49–56. [[CrossRef](#)] [[PubMed](#)]
13. Zhou, X.-Q.; Busemann, A.; Meijer, M.S.; Siegler, M.A.; Bonnet, S. The Two Isomers of a Cyclometalated Palladium Sensitizer Show Different Photodynamic Properties in Cancer Cells. *Chem. Commun.* **2019**, *55*, 4695–4698. [[CrossRef](#)] [[PubMed](#)]
14. Turnbull, W.L.; Luyt, L.G. Amino-Substituted 2,2'-Bipyridine Ligands as Fluorescent Indicators for ZnII and Applications for Fluorescence Imaging of Prostate Cells. *Chem. Eur. J.* **2018**, *24*, 14539–14546. [[CrossRef](#)] [[PubMed](#)]
15. Borges da Silva, R.; Teixeira, R.I.; Wardell, J.L.; Wardell, S.M.S.V.; Garden, S.J. Copper(ii) Catalyzed Synthesis of Novel Helical Luminescent Benzo[4,5]imidazo[1,2-a][1,10]phenanthrolines via an Intramolecular C–H Amination Reaction. *Org. Biomol. Chem.* **2017**, *15*, 812–826. [[CrossRef](#)]
16. Otani, T.; Tsuyuki, A.; Iwachi, T.; Someya, S.; Tateno, K.; Kawai, H.; Saito, T.; Kanyiva, K.S.; Shibata, T. Facile Two-Step Synthesis of 1,10-Phenanthroline-Derived Polyaza[7]Helicenes with High Fluorescence and CPL Efficiency. *Angew. Chem. Int. Ed.* **2017**, *56*, 3906–3910. [[CrossRef](#)]

17. Ding, S.; Wang, L.; Miao, Z.; Li, P. NNB-Type Tridentate Boryl Ligands Enabling a Highly Active Iridium Catalyst for C–H Borylation. *Molecules* **2019**, *24*, 1434. [[CrossRef](#)]
18. Otani, T.; Sasayama, T.; Iwashimizu, C.; Kanyiva, K.S.; Kawai, H.; Shibata, T. Short-Step Synthesis and Chiroptical Properties of Polyaza[5]–[9]Helicenes with Blue to Green-Colour Emission. *Chem. Commun.* **2020**, *56*, 4484–4487. [[CrossRef](#)] [[PubMed](#)]
19. Kim, D.; Ghosh, P.; Kwon, N.Y.; Han, S.H.; Han, S.; Mishra, N.K.; Kim, S.; Kim, I.S. Deoxygenative Amination of Azine- N -Oxides with Acyl Azides via [3+2] Cycloaddition. *J. Org. Chem.* **2020**, *85*, 2476–2485. [[CrossRef](#)] [[PubMed](#)]
20. Cheon, J.-D.; Mutai, T.; Araki, K. Preparation of a Series of Novel Fluorophores, N-Substituted 6-Amino and 6,6''-Diamino-2,2':6',2''-Terpyridine by Palladium-Catalyzed Amination. *Tetrahedron Lett.* **2006**, *47*, 5079–5082. [[CrossRef](#)]
21. Kopchuk, D.S.; Chepchugov, N.V.; Kovalev, I.S.; Santra, S.; Rahman, M.; Giri, K.; Zyryanov, G.V.; Majee, A.; Charushin, V.N.; Chupakhin, O.N. Solvent-Free Synthesis of 5-(Aryl/Alkyl)Amino-1,2,4-Triazines and α -Arylamino-2,2'-Bipyridines with Greener Prospects. *RSC Adv.* **2017**, *7*, 9610–9619. [[CrossRef](#)]
22. Kopchuk, D.S.; Krinochkin, A.P.; Starnovskaya, E.S.; Shtaitz, Y.K.; Khasanov, A.F.; Taniya, O.S.; Santra, S.; Zyryanov, G.V.; Majee, A.; Rusinov, V.L.; et al. 6-Arylamino-2,2'-Bipyridine “Push-Pull” Fluorophores: Solvent-Free Synthesis and Photophysical Studies. *ChemistrySelect* **2018**, *3*, 4141–4146. [[CrossRef](#)]
23. Kopchuk, D.S.; Starnovskaya, E.S.; Shtaitz, Y.K.; Khasanov, A.F.; Kim, G.A.; Nosova, E.V.; Krinochkin, A.P.; Zyryanov, G.V.; Rusinov, V.L.; Chupakhin, O.N. 5-Aryl-2,2'-Bipyridines Bearing Fluorinated Anilines Residues at C6 Position: Synthesis and Photophysical Properties. *Res. Chem. Intermed.* **2020**, *46*, 3929–3944. [[CrossRef](#)]
24. Starnovskaya, E.S.; Savchuk, M.I.; Shtaitz, Y.K.; Kopchuk, D.S.; Kovalev, I.S.; Pavlyuk, D.E.; Khasanov, A.F.; Zyryanov, G.V.; Chupakhin, O.N. Polynuclear Aromatic Amines as N-Nucleophiles in the Ipso-Substitution of the Cyano Group in 1,2,4-Triazines. *Russ. J. Org. Chem.* **2020**, *56*, 335–338. [[CrossRef](#)]
25. Starnovskaya, E.S.; Kopchuk, D.S.; Khasanov, A.F.; Tanya, O.S.; Santra, S.; Giri, K.; Rahman, M.; Kovalev, I.S.; Zyryanov, G.V.; Majee, A.; et al. Synthesis and Photophysics of New Unsymmetrically Substituted 5,5'-Diaryl-2,2'-Bipyridine-Based “Push-Pull” Fluorophores. *Dye. Pigment.* **2019**, *162*, 324–330. [[CrossRef](#)]
26. Kopchuk, D.S.; Chepchugov, N.V.; Starnovskaya, E.S.; Khasanov, A.F.; Krinochkin, A.P.; Santra, S.; Zyryanov, G.V.; Das, P.; Majee, A.; Rusinov, V.L.; et al. Synthesis and Optical Properties of New 2-(5-Arylpyridine-2-Yl)-6-(Het)Arylquinoline-Based “Push-Pull” Fluorophores. *Dye. Pigment.* **2019**, *167*, 151–156. [[CrossRef](#)]
27. Lakowicz, J.R. *Principles of Fluorescence Spectroscopy*, 3rd ed.; Lakowicz, J.R., Ed.; Springer: Boston, MA, USA, 2006; ISBN 978-0-387-31278-1.
28. Lippert, E. Spektroskopische Bestimmung Des Dipolmomentes Aromatischer Verbindungen Im Ersten Angeregten Singulettzustand. *Electro. Chem.* **1957**, *61*, 962–975.
29. Mataga, N.; Kaifu, Y.; Koizumi, M. Solvent Effects upon Fluorescence Spectra and the Dipolemoments of Excited Molecules. *Bull. Chem. Soc. Jpn.* **1956**, *29*, 465–470. [[CrossRef](#)]
30. Moseev, T.D.; Nikiforov, E.A.; Varaksin, M.V.; Starnovskaya, E.S.; Savchuk, M.I.; Nikonov, I.L.; Kopchuk, D.S.; Zyryanov, G.V.; Chupakhin, O.N.; Charushin, V.N. Novel Pentafluorophenyl- and Alkoxyphenyl-Appended 2,2'-Bipyridine Push–Pull Fluorophores: A Convenient Synthesis and Photophysical Studies. *Synthesis* **2021**, *53*, 3597–3607. [[CrossRef](#)]
31. Kosower, E.M. *Introduction to Physical Organic Chemistry Hardcover*; John Wiley & Sons: Hoboken, NJ, USA, 1968; Volume 1.
32. Kosower, E.M. The Effect of Solvent on Spectra. I. A New Empirical Measure of Solvent Polarity: Z-Values. *J. Am. Chem. Soc.* **1958**, *80*, 3253–3260. [[CrossRef](#)]
33. Reichardt, C. Solvatochromic Dyes as Solvent Polarity Indicators. *Chem. Rev.* **1994**, *94*, 2319–2358. [[CrossRef](#)]
34. Reichardt, C. *Solvents and Solvent Effects in Organic Chemistry*, 3rd, Updated and Enlarged Edition; Wiley-VCH Verlag GmbH & Co. KGaA: Weinheim, Germany, 2006.
35. Kovács, S.L.; Nagy, M.; Fehér, P.P.; Zsuga, M.; Kéki, S. Effect of the Substitution Position on the Electronic and Solvatochromic Properties of Isocyanaminonaphthalene (ICAN) Fluorophores. *Molecules* **2019**, *24*, 2434. [[CrossRef](#)]
36. Ertl, P. A Web Tool for Calculating Substituent Descriptors Compatible with Hammett Sigma Constants. *ChemRxiv* **2021**. [[CrossRef](#)]
37. Frisch, M.J.; Trucks, G.W.; Schlegel, H.B.; Scuseria, G.E.; Robb, M.A.; Cheeseman, J.R.; Scalmani, G.; Barone, V.; Petersson, G.A.; Nakatsuji, H.; et al. *Gaussian 09, Revision C.01*; Gaussian, Inc.: Wallingford, CT, USA, 2010.
38. Grabowski, Z.R.; Rotkiewicz, K.; Rettig, W. Structural Changes Accompanying Intramolecular Electron Transfer: Focus on Twisted Intramolecular Charge-Transfer States and Structures. *Chem. Rev.* **2003**, *103*, 3899–4032. [[CrossRef](#)]
39. Germain, M.E.; Knapp, M.J. Optical Explosives Detection: From Color Changes to Fluorescence Turn-On. *Chem. Soc. Rev.* **2009**, *38*, 2543. [[CrossRef](#)]
40. Verbitskiy, E.V.; Rusinov, G.L.; Chupakhin, O.N.; Charushin, V.N. Design of Fluorescent Sensors Based on Azaheterocyclic Push-Pull Systems towards Nitroaromatic Explosives and Related Compounds: A Review. *Dye. Pigment.* **2020**, *180*, 108414. [[CrossRef](#)]
41. Kozhevnikov, V.N.; Kozhevnikov, D.N.; Nikitina, T.V.; Rusinov, V.L.; Chupakhin, O.N.; Zabel, M.; König, B. A Versatile Strategy for the Synthesis of Functionalized 2,2'-Bi- and 2,2':6',2''-Terpyridines via Their 1,2,4-Triazine Analogues. *J. Org. Chem.* **2003**, *68*, 2882–2888. [[CrossRef](#)]
42. Dolomanov, O.V.; Bourhis, L.J.; Gildea, R.J.; Howard, J.A.K.; Puschmann, H. OLEX2: A Complete Structure Solution, Refinement and Analysis Program. *J. Appl. Crystallogr.* **2009**, *42*, 339–341. [[CrossRef](#)]

43. Sheldrick, G.M. SHELXT—Integrated Space-Group and Crystal-Structure Determination. *Acta Crystallogr. A Found. Adv.* **2015**, *71*, 3–8. [[CrossRef](#)] [[PubMed](#)]
44. Marenich, A.V.; Cramer, C.J.; Truhlar, D.G. Universal Solvation Model Based on Solute Electron Density and on a Continuum Model of the Solvent Defined by the Bulk Dielectric Constant and Atomic Surface Tensions. *J. Phys. Chem. B* **2009**, *113*, 6378. [[CrossRef](#)] [[PubMed](#)]